Available online at www.sciencedirect.com
ScienceDirect
Journal of Power Sources 159 (2006) 1468–1473
JOURNAL OF POWER SOURCES
www.elsevier.com/locate/jpowsour

Improved rechargeability of manganese oxide cathodes in alkaline cells in the presence of TiB_2 and TiS_2

V. Raghuveer, A. Manthiram *

Materials Science and Engineering Program, The University of Texas at Austin, Austin, TX 78712, United States

Received 7 November 2005; received in revised form 4 December 2005; accepted 5 December 2005
Available online 24 January 2006

Abstract

The rechargeability of electrolytic manganese dioxide (EMD) cathodes in the presence of small amounts (<5 wt.%) of TiB_2 and TiS_2 additives has been investigated in alkaline cells in the one electron regime and the data are compared with those obtained with the already known Bi_2O_3 additive. Both the TiB_2 and TiS_2 additives are found to offer slightly better cyclability at higher number of cycles compared to the Bi_2O_3 additive. However, the incorporation of small amounts of TiB_2 or TiS_2 into the Bi_2O_3 additive leads to a significant improvement in the cyclability compared to the Bi_2O_3 additive, possibly due to a synergistic effect. X-ray diffraction patterns recorded before and after 30 cycles as well as cyclic voltammograms recorded after 3 and 30 cycles reveal that the better cyclability in the presence of TiB_2 and TiS_2 additives is due to the suppression of the formation of unwanted, electrochemically inactive birnessite and hausmannite phases and a shifting of the second electron capacity of Mn to higher potentials.

Keywords: Alkaline batteries; Manganese oxide cathode; Chemical additives; Electrochemical properties

1. Introduction

Rechargeable alkaline batteries based on electrolytic manganese dioxide (EMD) cathodes are appealing as they offer a safe, environmentally benign, low cost system with high capacity involving theoretically two electrons per Mn. EMD (γ-MnO_2) is composed of intergrowths of pyrolusite (β-MnO_2) and ramsdellite domains that are characterized by, respectively, 1×1 and 1×2 tunnels [1]. However, EMD is plagued by poor rechargeability [3–11]. An important breakthrough was made by Wroblowa et al. [12–14] in the mid-1980s by incorporating significant amounts (>5 wt.%) of Bi_2O_3 into EMD, which improved the rechargeability significantly. Recently, our group [15–17] showed from an X-ray diffraction analysis of the cycled EMD cathodes in the one electron regime that part of the capacity fading is due to the formation of electrochemically inactive phases such as birnessite and hausmannite (Mn_3O_4). Designed chemical reaction experiments indicated that the formation of such electrochemically inactive phases is due to the chemical instability of the reduced form (δ-MnOOH) of EMD. The dissolution and subsequent disproportionation of the Mn^{3+} ions are responsible for the formation of the unwanted birnessite and hausmannite phases. Incorporation of Bi- or Ba-containing compounds into the cathode was found to suppress the formation of such inactive phases by keeping the Mn^{3+} ions in solution for longer times without disproportionation.

Following the incorporation of the Bi^{3+} additive, several other additives have been explored [18–22]. A potential candidate in this regard has been Ti^{4+} ion [23]. The incorporation of Ti^{4+} ion into EMD is usually carried out by an anodic deposition of EMD from an acidic solution of manganese sulfate containing some Ti^{4+} ions. We present here the incorporation of small amounts (<2 wt.%) of TiB_2 and TiS_2 additives into EMD by physical mixing and an investigation of their electrochemical behavior.

2. Experimental

Commercially available EMD (from Chemmetals) and TiB_2, TiS_2, and Bi_2O_3 (all from Alfa Aesar) were used in this study. Thin film type electrodes containing 5–8 mg of the active material were prepared by mixing 75 wt.% modified EMD consisting of 0.5–5 wt.% TiB_2, TiS_2, $Bi_2O_3 + TiB_2$, or $Bi_2O_3 + TiS_2$ additive with 20 wt.% graphite (Timrex SFG-15) and 5 wt.%

* Corresponding author. Tel.: +1 512 471 1791; fax: +1 512 471 7681.
E-mail address: rmanth@mail.utexas.edu (A. Manthiram).

0378-7753/$ – see front matter © 2005 Elsevier B.V. All rights reserved.
doi:10.1016/j.jpowsour.2005.12.005

polytetrafluoroethylene (PTFE) binder in a mortar and pestle, followed by rolling the mixture into thin sheets. The thin film electrode was then mounted onto a nickel mesh current collector. The electrochemical measurements were carried out with a three-electrode assembly using a Hg/HgO (in 9 M KOH) reference electrode, a porous nickel counter electrode consisting of $NiOOH/Ni(OH)_2$, and 9 M KOH electrolyte. The cycling experiments were carried out under constant current discharge/charge conditions between −0.4 and +0.35 V versus Hg/HgO with discharge and charge rates of, respectively, *C*/2 and *C*/4. The slow-scan cyclic voltammograms were recorded in the range of −1.0 to +0.35 V versus Hg/HgO at a scan rate of 40 $\mu V\,s^{-1}$ without leaving any rest period between cycles. Structural characterizations of the cathodes before and after the electrochemical tests was carried out with X-ray diffraction. The cycled cathodes were washed with deionized water and dried under vacuum at room temperature overnight before examining by X-ray diffraction.

3. Results and discussion

Fig. 1 compares the cyclabilities of EMD containing various amounts of TiB_2 (0.5–5 wt.%) (Fig. 1a) and TiS_2 (0.5–2 wt.%) (Fig. 1b) additives with those of plain EMD and EMD containing

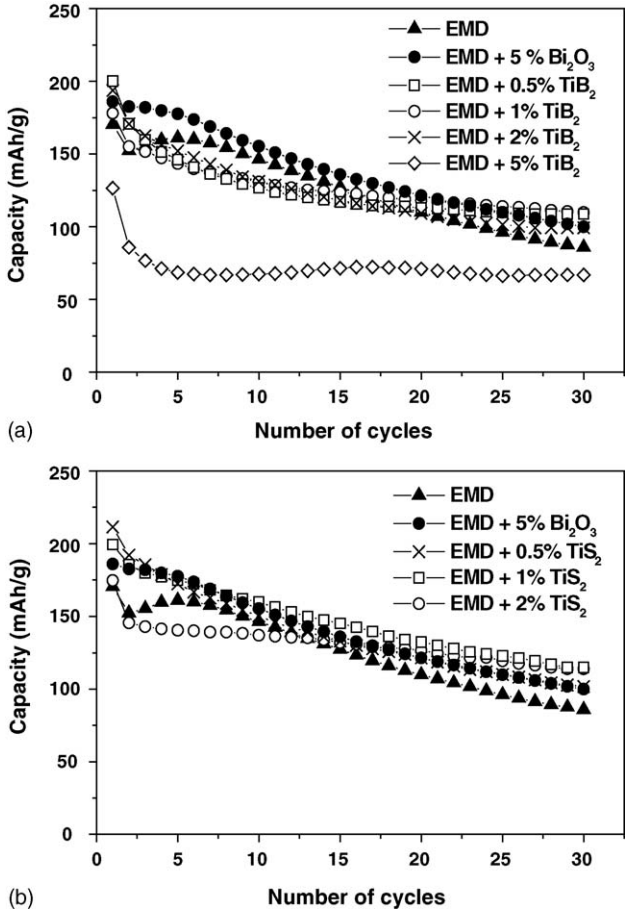

Fig. 1. Comparison of the cyclability of EMD in the presence of various amounts of (a) TiB_2 (0.5–5 wt.%) and (b) TiS_2 (0.5–2 wt.%) additives with those of plain EMD and EMD with 5 wt.% Bi_2O_3 additive.

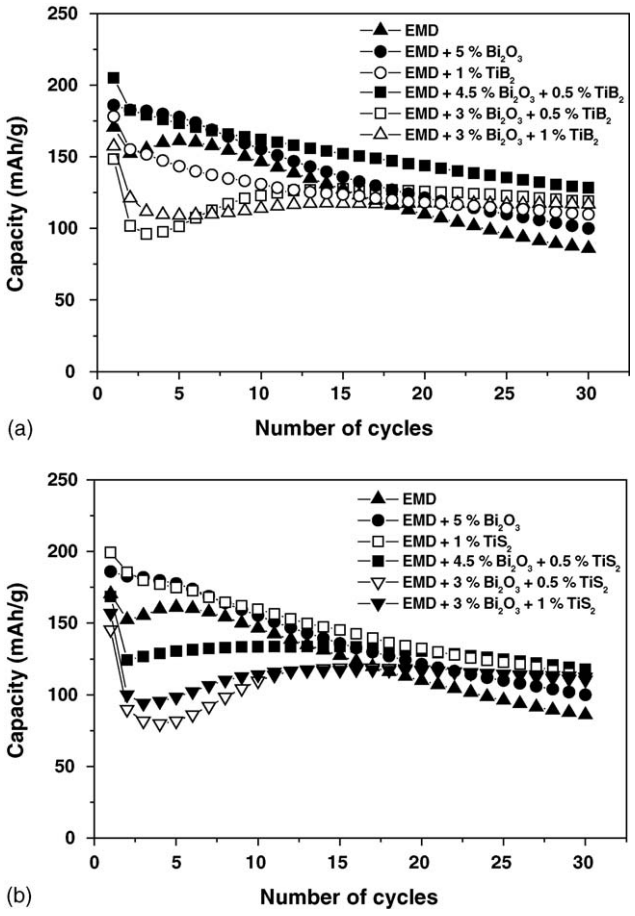

Fig. 2. Comparison of the cyclability of EMD in the presence of various amounts/ratios of (a) $Bi_2O_3 + TiB_2$ and (b) $Bi_2O_3 + TiS_2$ additives with those of plain EMD and EMD with 5 wt.% Bi_2O_3 additive.

5 wt.% Bi_2O_3. The TiB_2 and TiS_2 additives give slightly better cyclability compared to the plain EMD or the Bi_2O_3 additive, particularly at higher number of cycles, suggesting an important benefit for long-term cycling. The capacity retention generally increases with increasing amount of additives, but at the expense of the capacity value. An optimum amount of 1 wt.% TiB_2 or TiS_2 offers the best combination of cyclability and capacity. Fig. 2 compares the cyclabilities of EMD containing various amounts of mixed $Bi_2O_3 + TiB_2$ and $Bi_2O_3 + TiS_2$ additives. The data indicate that the addition of small amounts (0.5 wt.%) of TiB_2 or TiS_2 along with the Bi_2O_3 additive leads to a significant improvement in cyclability compared to the individual Bi_2O_3, TiB_2, or TiS_2 additives, possibly due to a synergistic effect.

With an aim to understand the origin of the better cyclability in the presence of TiB_2 and TiS_2 additives with and without Bi_2O_3, we have focused on a comparison of the structural characterization of the cathodes before and after cycling. Fig. 3 compares the X-ray diffraction patterns of the cathodes with and without various additives before and after 30 cycles in the one electron-region (cathodic cut-off potential: −0.4 V versus Hg/HgO). While reflections corresponding to birnessite (δ-MnO_2) and hausmannite (Mn_3O_4) phases are found in the cycled cathodes consisting of plain EMD (Fig. 3b) and EMD +5 wt.%

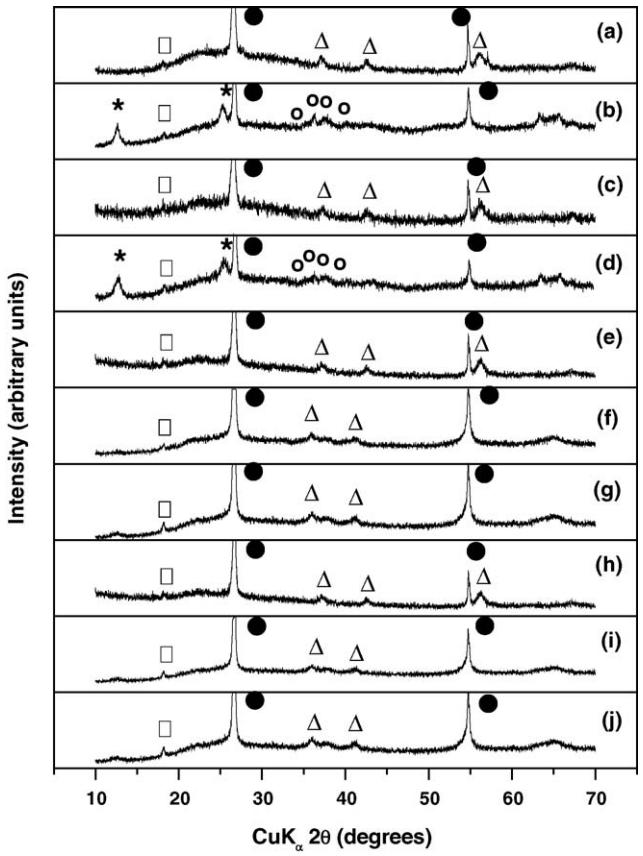

Fig. 3. X-ray diffraction patterns recorded in the charged state before and after 30 cycles: (a) plain EMD before cycling, (b) plain EMD after 30 cycles, (c) EMD with 5 wt.% Bi_2O_3 before cycling, (d) EMD with 5 wt.% Bi_2O_3 after 30 cycles, (e) EMD with 1 wt.% TiB_2 before cycling, (f) EMD with 1 wt.% TiB_2 after 30 cycles, (g) EMD with 4.5 wt.% Bi_2O_3 + 0.5 wt.% TiB_2 after 30 cycles, (h) EMD with 1 wt.% TiS_2 before cycling, (i) EMD with 1 wt.% TiS_2 after 30 cycles, and (j) EMD with 4.5 wt.% Bi_2O_3 + 0.5 wt.% TiS_2 after 30 cycles. ●, □, △, ⋆ and **O** refer to graphite, PTFE, γ-MnO_2, birnessite, and hausmannite, respectively. The slight shift in the peak positions of γ-MnO_2 observed in part (f), (g), (i), and (j) could be due to the partial incorporation of H^+ into the MnO_2 lattice.

Bi_2O_3 (Fig. 3d), no such reflections are found in the cycled cathodes consisting of EMD and small amounts (≤1 wt.%) of TiB_2 or TiS_2 additives in the absence (Fig. 3f and i) and presence (Fig. 3g and j) of Bi_2O_3. Thus the better cyclability in the presence of TiB_2 or TiS_2 additives with and without the Bi_2O_3 additive at higher number of cycles is related to the effective suppression of the formation of the electrochemically inactive birnessite and hausmannite phases [15–22].

In order to understand the redox process, we have compared the slow-scan cyclic voltammograms (CV) of the cathodes with and without the various additives after 3 and 30 discharge–charge cycles and the CV profiles are shown in Fig. 4. The redox processes of plain EMD (Fig. 4a) and EMD in the presence of Bi_2O_3 (Fig. 4c and d) are in general agreement with that reported before in the literature [23–25]. The two cathodic peaks C_1 and C_2 correspond, respectively, to the homogeneous reduction of Mn^{4+} to Mn^{3+} and the heterogeneous reduction of Mn^{3+} to Mn^{2+} and the two anodic peaks A_1 (∼−0.16 V) and A_2 (∼+0.17 V) correspond, respectively, to the oxidation of Mn^{2+} to Mn^{3+} and Mn^{3+} to Mn^{4+}. However, although the nature of the CVs obtained in the presence of 1 wt.% TiB_2 (Fig. 4e and f) and 1 wt.% TiS_2 (Fig. 4g and h) is similar to those of EMD (Fig. 4a) and Bi_2O_3-modified EMD (Fig. 4c), the observed shift in the cathodic (C_1) and anodic (A_1 and A_2) peak potentials and the characteristically narrow peaks may suggest slight changes in the nature of the intermediates formed during the reduction process in the presence of TiB_2 and TiS_2.

To develop a further understanding, we have also focused on a comparison of the contribution of the percentage (%) two-electron capacity based on the slow-scan cyclic voltammograms in Fig. 4. The percentage (%) two-electron capacity is defined as the ratio of charge associated with the cathodic peak C_1 (corresponds to the reduction of Mn^{4+} to Mn^{3+}) and the anodic peaks A_1 and A_2 (correspond to the two-step oxidation of Mn^{2+} to Mn^{4+}). After three cycles, plain EMD has a % two-electron capacity value of 50 (Fig. 4a) since all of the second electron reduction (Mn^{3+} to Mn^{2+} and peak C_2) takes place at a far negative potential, viz., −0.5 to −0.8 V and its contribution at a cut-off potential of ≥−0.4 V is not available. On the other hand, the cathode with 5 wt.% Bi_2O_3 has a % two-electron capacity value of 74 above a potential of ≥−0.6 V with a broad peak for C_1 (Fig. 4c) after three cycles, indicating the availability of part of the second electron capacity at cut-off potentials of ≥−0.4 V. Thus the slightly higher discharge capacity value (better cyclability) of the cathode containing Bi_2O_3 is due to the shifting to and availability at a higher voltage of the second electron capacity, which is in agreement with the previous reports [21–27].

The cathodes containing 1 wt.% TiB_2 (Fig. 4e) and TiS_2 (Fig. 4g) show during cathodic sweep a shoulder peak at −0.45 to −0.5 V along with the cathodic peak C_1 at −0.2 to −0.45 V after three cycles. With the peak C_1 and the shoulder peak, these cathodes have % two-electron capacity values of 65 (1 wt.% TiB_2) and 57 (1 wt.% TiS_2) after three cycles (Fig. 4e and g), which are lower than that found with 5 wt.% Bi_2O_3 (Fig. 4c). The difference as well as the lower initial capacity values observed for the TiB_2 and TiS_2 modified EMD in Figs. 1 and 2 could be due to the availability of a lower percentage of the second electron contribution at a potential ≥−0.4 V (cathodic cut-off voltage: −0.4 V) compared to that with the Bi_2O_3 additive.

The cathodes (in the presence and absence of additives) after subjecting to 30 discharge–charge cycles in the one electron regime (cut-off voltage: −0.4 V) show CV behaviors significantly different from those observed with the cathodes cycled for 3 cycles (Fig. 4). For example, plain EMD shows lower current for peak C_1 and lower % two-electron capacity after 30 cycles with a significant change in the shape and features of CV (Fig. 4b) compared to that after 3 cycles, which could be due to the formation of electrochemically inactive phases (Fig. 3), resulting in a continuous capacity fade in Fig. 1. On the other hand, in the presence of Bi_2O_3 additive, the unresolved cathodic peak C_1 observed after 3 cycles (Fig. 4c) becomes resolved into two peaks after 30 cycles (Fig. 4d), which is consistent with the previous literature report [2]. Although the % two-electron capacity value (72) above a potential of ≥−0.6 V found after

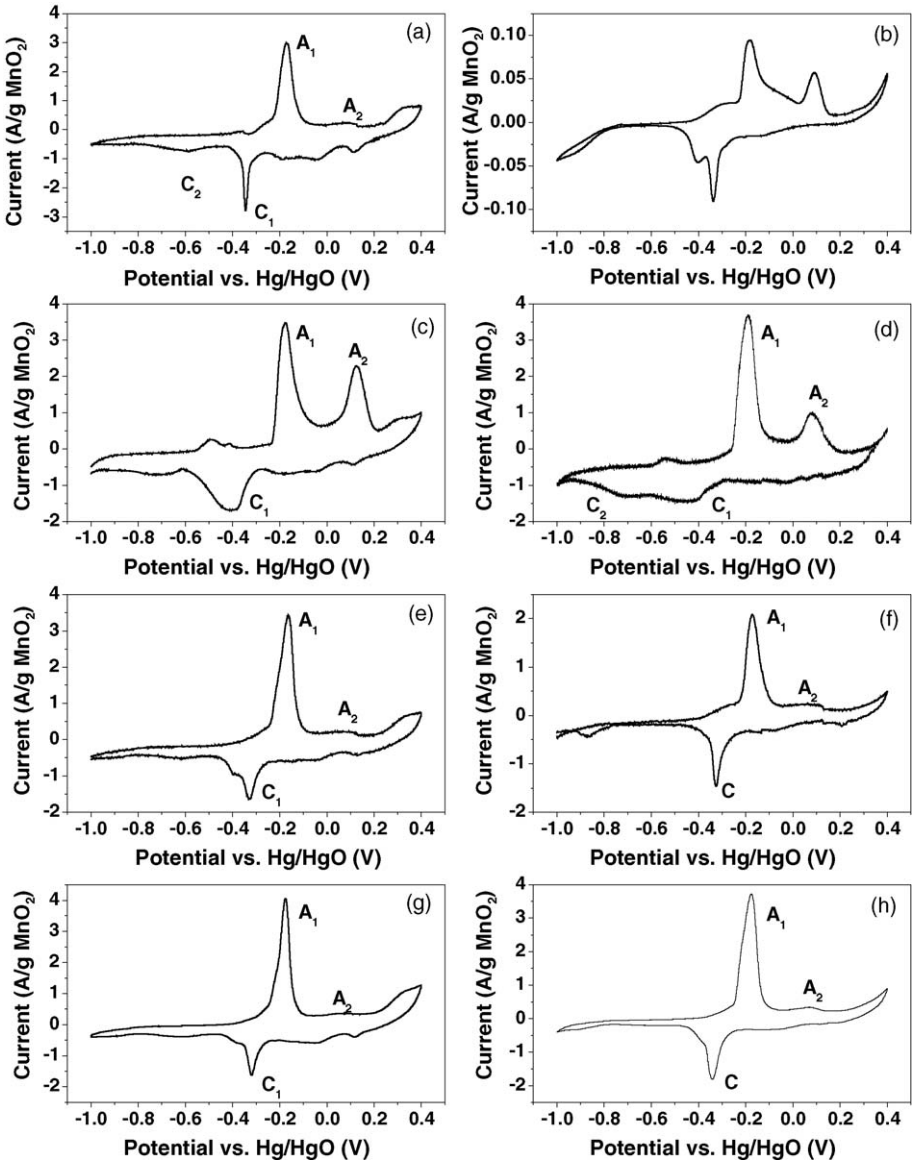

Fig. 4. Cyclic voltammograms (CV) recorded in 9 M KOH at a sweep rate of 4×10^{-5} V s^{-1} after cycling the electrodes galvanostatically in the one electron-region (cut-off charge voltage: −0.4 V vs. Hg/HgO): (a) plain EMD after three cycles, (b) plain EMD after 30 cycles, (c) EMD with 5 wt.% Bi_2O_3 after three cycles, (d) EMD with 5 wt.% Bi_2O_3 after 30 cycles, (e) EMD with 1% TiB_2 after three cycles, (f) EMD with 1% TiB_2 after 30 cycles, (g) EMD with 1% TiS_2 after three cycles, and (h) EMD with 1% TiS_2 after 30 cycles.

30 cycles does not change much compared to that found after 3 cycles (74), the formation of inactive birnessite and hausmannite phases decreases the reversible capacity. Thus the benefit provided by the Bi_2O_3 additive decreases with cycling, resulting in a continuous capacity fade on cycling the cathodes at ≥ -0.4 as seen in Figs. 1 and 2.

In the presence of 1 wt.% TiB_2 and TiS_2 additives, the shoulder peaks observed at −0.45 to −0.5 V after 3 cycles (Fig. 4e and g) become nearly unresolved by getting merged with the cathodic peak at −0.4 V after 30 cycles (Fig. 4f and h). This shift in the second electron reduction potential may be due to the surface modification of EMD or the changes in the nature of the Mn^{3+} intermediates formed in the presence of TiB_2 and TiS_2 during the course of cycling. With the peak C_1 and the shoulder peak together, these cathodes have % two-electron capacity values of 60 (1 wt.% TiB_2) and 57 (1 wt.% TiS_2) after 30 cycles (Fig. 4f and h). In other words, the second electron capacity can be utilized partly in the case of TiB_2 and TiS_2 modified EMD at an almost single-valued potential, viz., −0.4 V versus Hg/HgO after extended cycling unlike in the case of Bi_2O_3 modified EMD, resulting in good capacity retention at higher number of cycles.

Fig. 5 compares the CV behaviors of the EMD cathodes containing $Bi_2O_3 + TiB_2$ and $Bi_2O_3 + TiS_2$ additives after 3 and 30 galvanostatic cycles in the one electron regime (cut-off voltage: −0.4 V). In the presence of $Bi_2O_3 + TiB_2$, a shoulder peak at −0.45 to −0.5 V along with the cathodic peak C_1 at −0.2 to −0.45 V is observed during the cathodic sweep after 3 cycles (Fig. 5a), while no such shoulder peak is observed in the case of the cathode containing $Bi_2O_3 + TiS_2$ additive (Fig. 5c). How-

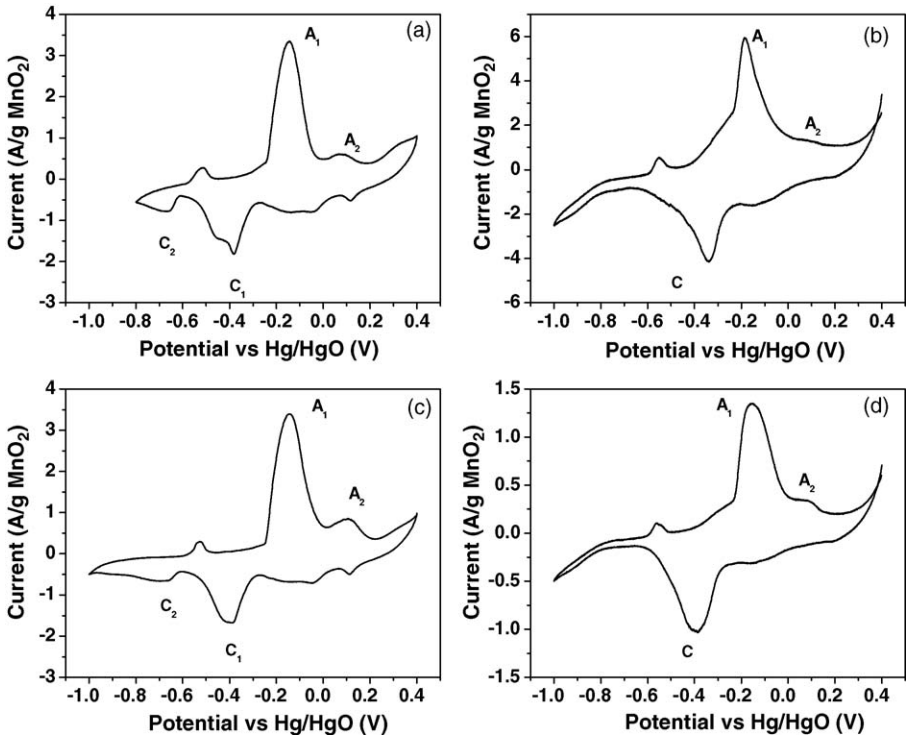

Fig. 5. Cyclic voltammograms (CV) recorded in 9 M KOH at a sweep rate of 4×10^{-5} V s^{-1} after cycling the electrodes galvanostatically in the one electron-region (cut-off charge voltage: −0.4 V vs. Hg/HgO): (a) EMD with 4.5 wt.% Bi_2O_3 + 0.5 wt.% TiB_2 after three cycles, (b) EMD with 4.5 wt.% Bi_2O_3 + 0.5 wt.% TiB_2 after 30 cycles, (c) EMD with 4.5 wt.% Bi_2O_3 + 0.5 wt.% TiS_2 after three cycles, and (d) EMD with 4.5 wt.% Bi_2O_3 + 0.5 wt.% TiS_2 after 30 cycles.

ever, the % two-electron capacity values of 67 ($Bi_2O_3 + TiB_2$) and 60 ($Bi_2O_3 + TiS_2$) found after 3 cycles (Fig. 5a and c) are lower than that found with 5 wt.% Bi_2O_3 (72) (Fig. 4c), which is consistent with the slightly lower initial capacity values observed in the presence of $Bi_2O_3 + TiB_2$ and $Bi_2O_3 + TiS_2$ additives as seen in Fig. 2. After subjecting to 30 discharge–charge cycles in the one electron regime, the resolved cathodic peak C_1 observed in the presence of $Bi_2O_3 + TiB_2$ (Fig. 5a) after 3 cycles becomes unresolved (Fig. 5b), while the unresolved peak C_1 observed in the presence of $Bi_2O_3 + TiS_2$ (Fig. 5c) after 3 cycles remains unresolved (Fig. 5d). However, the cathodes have a % two-electron capacity values of 72 and 67 in the presence of, respectively, the $Bi_2O_3 + TiB_2$ and $Bi_2O_3 + TiS_2$ additives after 30 cycles (Fig. 5b and d), indicating that the second electron capacity is available even after extended cycling. The maintenance of the second electron capacity even after extended cycling could be responsible for the observed enhancement in the rechargeability (Fig. 2).

Furthermore, the observations made with the $Bi_2O_3 + TiB_2$ and $Bi_2O_3 + TiS_2$ additives is in contrast to that made with the Bi_2O_3 additive alone, where the unresolved cathodic peak C_1 observed after 3 cycles (Fig. 4c) becomes resolved into two peaks after 30 cycles (Fig. 4d), resulting in a lowering of the second electron capacity at higher potentials after 30 cycles and consequently a capacity fade on extended cycling. The data thus reveal that the presence of TiB_2 or TiS_2 in the mixed $Bi_2O_3 + TiB_2$ and $Bi_2O_3 + TiS_2$ additives is essential to shift the second electron capacity and make it available at higher potentials, offering good cyclability in the one electron regime.

4. Conclusions

The incorporation of small amounts (<5 wt.%) of TiB_2 and TiS_2 additives into EMD is found to improve the rechargeability slightly in the one electron regime, particularly at higher number of cycles, compared to that found with the previously known additive Bi_2O_3. On the other hand, incorporation of small amounts of TiB_2 or TiS_2 into the Bi_2O_3 additive improves the rechargeability significantly compared to the individual Bi_2O_3, TiB_2, or TiS_2 additives. The enhanced rechargeability is found to be due to the suppression of the formation of unwanted, electrochemically inactive birnessite and hausmannite phases and the shifting of the second electron capacity to higher potentials as the cathode is cycled. The study demonstrates that identification of potential additives through a systematic investigation could enhance the commercial feasibility of rechargeable alkaline cells based on the inexpensive and environmentally benign manganese oxide cathodes.

Acknowledgments

Financial support by the Texas Higher Education Coordinating Board (Technology Development and Transfer grant 003658-0582-2003) and RBC Technologies is gratefully acknowledged.

References

[1] P.M. De Wolff, Acta Cryst. 12 (1959) 341.
[2] J. McBreen, Electrochim. Acta 20 (1975) 221.

[3] R. Patrice, B. Gerand, J.B. Lerische, L. Seguin, E. Wang, R. Moses, K. Brandt, J.N. Tarascon, J. Electrochem. Soc. 148 (2001) A448.
[4] K. Kordesch, J. Gsellmann, M. Peri, K. Tomantschger, R. Chemelli, Electrochim. Acta 26 (1981) 1495.
[5] K. Kordesch, M. Weissenbacher, J. Power Sources 51 (1994) 61.
[6] Y.W. Shen, K. Kordesch, J. Power Sources 87 (2000) 162.
[7] A. Kozawa, R.A. Powers, J. Electrochem. Soc. 113 (1966) 870.
[8] Y. Chabre, J. Pannetier, Prog. Solid Sate Chem. 23 (1995) 1.
[9] C. Mondoloni, M. Laborde, J. Rioux, E. Andoni, C. Levy-Clement, J. Electrochem. Soc. 139 (1992) 954.
[10] D. Boden, C.J. Venuto, D. Wisler, R.B. Wylie, J. Electrochem. Soc. 114 (1967) 415.
[11] C. Mondoloni, M. Laborde, J. Rioux, E. Andoni, C. Levy-Clement, J. Electrochem. Soc. 139 (1992) 954.
[12] Y.F. Yao, N. Gupta, H.S. Wroblowa, J. Electroanal. Chem. 223 (1987) 107.
[13] M.A. Dzieciuch, N. Gupta, H.S. Wroblowa, J. Electrochem. Soc. 135 (1988) 2415.
[14] H.S. Wroblowa, N. Gupta, J. Electroanal. Chem. 238 (1987) 98.
[15] A.M. Kannan, S. Bhavaraju, F. Prado, M. Manivel Raja, A. Manthiram, J. Electrochem. Soc. 149 (2002) A483.
[16] D. Im, A. Manthiram, J. Electrochem. Soc. 150 (2003) A68.
[17] D. Im, A. Manthiram, B. Coffey, J. Electrochem. Soc. 150 (2003) A1651.
[18] J.E. Mieczkowzka, P.S. Markfort, US Patent 5,342,712 (1993).
[19] W.M. Swierbut, J.C. Nardi, US Patent 5,501,924 (1996).
[20] M.F. Mansuetto, US Patent 6,524,750 (2003).
[21] V. Raghuveer, A. Manthiram, Electrochem. Commun. 7 (2005) 1329.
[22] S.W. Donne, G.A. Lawrance, D.A.J. Swinkels, J. Electrochem. Soc. 144 (1997) 2949.
[23] L. Bai, D.Y. Qui, B.E. Conway, Y.H. Zhou, G. Chowdhury, W.A. Adams, J. Electrochem. Soc. 140 (1993) 884.
[24] C.G. Castledine, B.E. Conway, J. Appl. Electrochem. 25 (1995) 707.
[25] S.W. Donne, G.A. Lawrance, D.A.J. Swinkels, J. Electrochem. Soc. 144 (1997) 2954.
[26] V.K. Nartey, L. Binder, A. Huber, J. Power Sources 87 (2000) 205.
[27] S.W. Donne, G.A. Lawrance, D.A.J. Swinkels, J. Electrochem. Soc. 144 (1997) 2961.